Pohl et al. Journal of the European Optical Society-Rapid Publications (2020) 16:19
https://doi.org/10.1186/s41476-020-00140-9

Journal of the European Optical Society-Rapid Publications

RESEARCH Open Access

# Mid-spatial frequency error generation mechanisms and prevention strategies for the grinding process

Mario Pohl[1*], Olga Kukso[2], Rainer Boerret[1] and Rolf Rascher[2]

## Abstract

The research presented in this paper is focused on the link between manufacturing parameters and the resulting mid-spatial frequency error in the manufacturing process of precision optics. The goal is to understand the generation mechanisms of mid-spatial frequency errors and avoid their appearance in the manufacturing process. Also, a simulation which is able to predict the resulting mid-spatial frequency error from a manufacturing process is developed and verified.

**Keywords:** Mid-spatial frequency error, MSFE, Ripple, Grinding, Optic manufacturing, Simulation

## Introduction

The classical manufacturing process of precision optics is based on a grinding and a polishing step. The quality parameters for the surface after the grinding step are shape, surface structure, roughness and sub surface damage (SSD). The errors in shape, surface structure and roughness can be considered as waviness with different surface wavelengths. The waviness can be classified as low-, mid- and high-spatial frequency error (LSFE, MSFE, HSFE). The LSFE represents shape errors and can be corrected with existing sub-aperture polishing techniques, for example, computer controlled polishing (CCP). The HSFE represents the roughness and can be smoothed for example by pad polishing. The MSFE is usually too large to be smoothed and too small to be corrected in a cost-efficient way. The MSFE can emerge in different states of the manufacturing process and its generation mechanisms are often not completely understood. The MSFE causes diffraction and decreases the image quality of an optical system. At the same time, optical components have to meet constantly rising requirements. Therefore, it is important to control the MSFE. This resembles a big challenge for the manufacturing process of precision optics. The demand for tools, techniques and strategies to avoid the MSFE is increasing [1–8].

There is no uniform definition of the exact range of the MSFE. This is because the MSFE range depends on each individual manufacturing process. In this research, all structures which are too large to be smoothed and too small, to be corrected in a cost-efficient way are considered as MSFE. It depends on the individual manufacturing process to determine which structures are too large to be smoothed or too small, to be corrected. Therefore different manufacturing processes have a different MSFE window [9].

The goal of this research is to develop a better understanding of the generation mechanisms of the MSFE. This should lead to techniques and strategies to avoid or at least decrease the appearance of the MSFE.

## Discussion

The same set of machine parameters in the same manufacturing process leads consistently to the same resulting MSFE on the surface of the manufactured part.

* Correspondence: mario.pohl@hs-aalen.de
[1]Aalen University of Applied Sciences, Center for Optical Technologies, 73430 Aalen, Germany
Full list of author information is available at the end of the article

Therefore, the generation of the MSFE is a deterministic process and should follow a defined model.

Periodic movements or vibrations during the manufacturing process are the root cause of the MSFE. The majority of these periodic movements or vibrations are related to the manufacturing parameters. Only very few of these movements or vibrations are constant and not related to the manufacturing parameters [10, 11].

Prior work has shown that the parameters of the grinding step have a significant impact on the resulting MSFE. After the grinding step, the MSFE usually consist of one dominating frequency and several residual frequencies, which are uniformly distributed along the grinding tool path. The residual frequencies are usually multiples of the main frequency. The main frequency can be linked directly to the path speed and the tool rotation during the grinding process [12–14].

Several series of experiments were carried out to proof this correlation. Figure 1 shows a surface measurement of two lenses after grinding. The lenses were ground with point-contact along a spiral path. In case of a constant rotation speed of the work piece, surface structures typically look as can be seen in Fig. 1 on the left side (A). In case of constant path speed, structures typically look as can be seen in Fig. 1 on the right side (B).

For both structures, the resulting MSFE frequency is equal to the quotient between tool rotation and path speed.

Figure 2 shows the amplitude frequency spectrum of a spherical sample (Ø 52 mm; radius of curvature 70 mm) after grinding at the top (A). The amplitude frequency spectrum of the same sample after polishing is shown at the bottom (B).

Figure 2 shows that, the amplitude of the main frequency was decreased by the polishing process but is still visible. The residual frequencies were smoothed out by the polishing steps. Therefore, according to the previous definition of MSFE, only the main frequency can be considered as in the MSFE range.

The spatial frequencies of the surface were obtained along the tool path of the grinding tool. This way the frequencies can be linked to the grinding parameters. The relevant grinding parameters for the sample are listed in Table 1.

The maximum of amplitude of the frequency peak, from the grinding process evaluated in Fig. 2, is found at a spatial frequency of about 0.41 1/mm. This is related to a spatial wavelength of about 2.44 mm. The path speed was at 12000 mm/min, and the tool rotation was at 5001 1/min. The path speed divided by the tool rotation equals about 2.4 mm. In other words, the time the tool needs to carry out one rotation, is the same time the tool needs to travel about 2.4 mm along the tool path. The tool rotation is directly printed on the surface in the form of a MSFE. Therefore, the MSFE generated by the grinding process can be directly linked to the tool rotation and the path speed.

$$spatial\ wavelenght = \frac{path\ speed}{tool\ rotation} \tag{1}$$

$$spatial\ frequency = \frac{1}{spatial\ wavelenght} \tag{2}$$

## Experiments

To build up a model of the generation mechanisms for the MSFE and to find strategies of avoidance, a wide

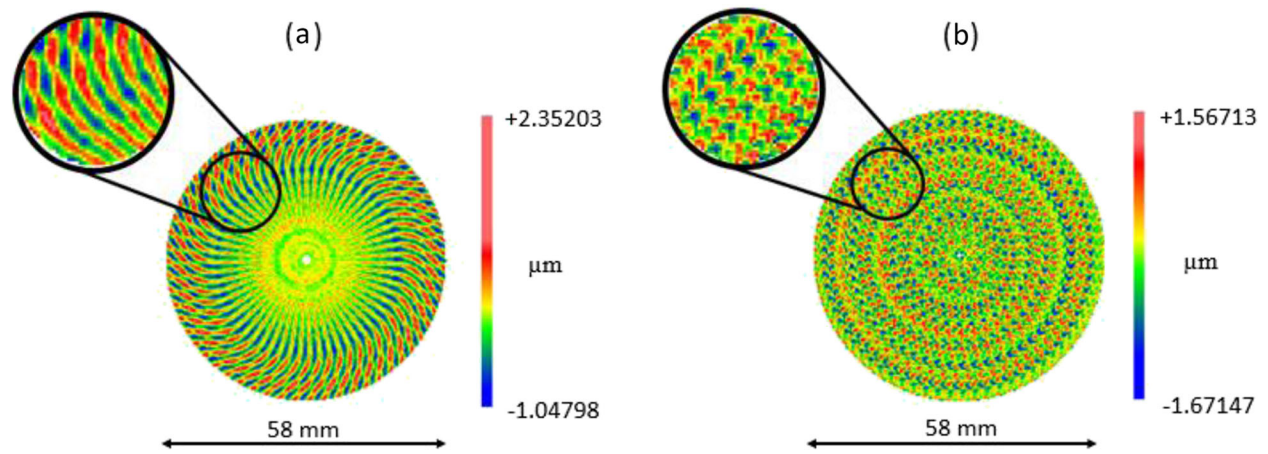


**Fig. 1** (**a**) False-colour plot of a tactile surface measurement of a sample, ground on a grinding machine SPM 140, with tool rotation 2971 1/min and sample rotation 50 1/min, path distance 0.05 mm; (**b**) False-colour plot of a tactile surface measurement of a sample, ground on a grinding machine SPM 140, with tool rotation 2971 1/min and path speed 5000 mm/min, path distance 0.05 mm. The first four Zernike coefficients were subtracted from both measurements. Machines, tools and substrate were used as described in Experiments section

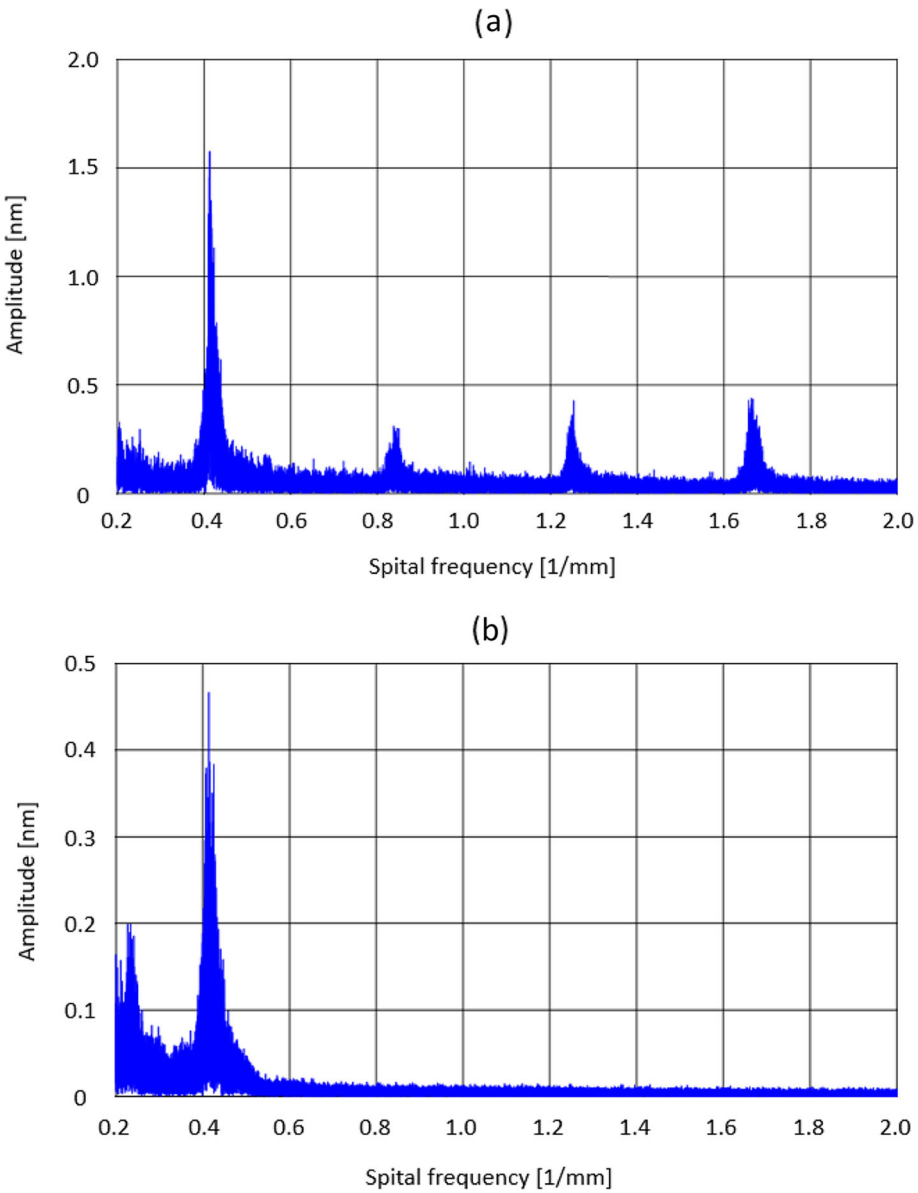


**Fig. 2** (**a**) Amplitude frequency spectrum of a ground sample; (**b**) Amplitude frequency spectrum of the same sample after polishing. The Frequencies are obtained along the grinding tool path and shifted into the frequency domain using Fourier transformation. The X-Axis shows the surface error as spatial frequencies (0.2 1/mm < spatial frequency < 2.0 1/mm). The Y-Axis shows the amplitude of the frequencies in nm. Fourier transformation: Normalized, unity window

**Table 1** Relevant grinding parameters of the sample evaluated in Fig. 2

| | |
|---|---|
| Kinematic mode: | Spiral tool path |
| Spiral distance: | 0.05 mm |
| Tool rotation speed: | 5001 1/min |
| Path speed: | 12,000 mm/min |

range of samples was manufactured and measured. During this experimental process, several different machines and tools were used for the grinding and polishing. All grinding experiments presented, were carried out on a Satisloh SPM 140 (point contact with 0.05 mm depth of cut, spiral mode with 0.05 mm path distance, constant path speed) with a wheel tool (D 15, BZM, C50). The radius of curvature of the tool was dressed to 60 mm before each series of experiments. All polishing experiments presented, were carried out on an Optotech MCP 250 (point contact, raster mode, constant path

speed) with a ball tool (Ø 70 mm, LP-26). All experiments presented, were carried out on a N-BK 7 glass substrate.

During the grinding of a plane sample, the rotation speed of the tool was changed several times. The goal was to determine the behaviour of the frequencies generated by the grinding process while the manufacturing parameters are changing. The measurement was obtained directly after the grinding process using a white light interferometer in stitching-mode. Afterwards, the measurements were evaluated along the tool path of the grinding tool.

The sample was ground with a path speed of 3000 mm/min. The different rotation speeds of the tool and the expected resulting spatial frequencies are listed in Table 2.

Figure 3 shows the amplitude frequency spectrum of the typical MSFE window of the ground sample.

The expected peaks (a), (b), (c) and (d) are clearly visible and can be well distinguished from the "noise". Peak (a) represents the biggest amplitude value after grinding and the peaks (b) and (c) are only slightly smaller in terms of amplitude. At peak (d), a further decrease in amplitude can be seen but it is still clearly distinguishable from the "noise". Peak (e) can only be distinguished from the "noise" because it is known where to look for it. The amplitude of peak (f) is too small to be distinguished from the "noise". Figure 4 shows a graph, which describes the behaviour of the amplitude of the MSFE-Peaks after grinding with respect to its spatial frequency.

The graph shows that with a further increase of the rotation speed of the tool the amplitude of the frequency generally decreases. Figure 5 shows the amplitude frequency spectrum of the typical MSFE window of the same sample after polishing.

It can be observed that, the frequency peaks (a), (b) and (c) are still visible after polishing. According to the previous definition, these remaining peaks can be considered the MSFE. The peaks (d), (e) and (f) are no longer visible after the polishing and can be considered removed from the surface. Therefore, according to the previous definition, these frequencies can be considered roughness. Peak (a) still represents the biggest amplitude value but the peaks (b) and (c) were only slightly lower after grinding. During the polishing, the amplitudes decreased differently.

**Table 2** Different rotation speeds of the tool and the expected resulting spatial frequency peaks for the experiment evaluated in Fig. 3

| Label | Tool rotation [1/min] | Expected frequency peak [1/mm] |
|---|---|---|
| (a) | 2207 | 0.736 |
| (b) | 3313 | 1.104 |
| (c) | 4007 | 1.336 |
| (d) | 5333 | 1.778 |
| (e) | 7121 | 2.374 |
| (f) | 9421 | 3.141 |

Figure 6 shows a graph, which describes the behaviour of the amplitude of the MSFE-Peaks after polishing with respect to its spatial frequency.

After the polishing, it can be observed that the amplitude of higher spatial frequencies is significantly more decreased than the amplitude of lower spatial frequencies. For lower spatial frequencies, the amplitude of the MSFE seems to remain higher during the polishing than for higher spatial frequencies.

To prove this result above, the following experiments were carried out:

Spherical samples with Ø 60 mm and a radius of curvature of 100 mm were ground. The used grinding parameters for each sample are displayed in Table 3. The tool generated MSFE frequency ranges from about 1.1 1/mm to 3.1 1/mm.

The ground surfaces were measured with a tactile device and analysed with Fourier transformation. Figure 7 shows the maximum of amplitude of the tool generated MSFE peak (A, B, C) and the mean value of all other significant maximums of amplitude in the spatial frequency interval between 0.5 and 4 1/mm (D, E, F) after grinding.

It can be seen that for tool generated MSFE frequencies with shorter wavelength, the amplitudes are equal or lower than the average MSFE from other sources. For frequencies with longer wavelength the tool generated MSFE is much higher in amplitude than the average MSFE from other sources and therefore dominating the MSFE range.

Afterwards the surfaces of the samples were polished. The polished surfaces were measured and analysed the same way as before. Figure 8 shows the maximum of amplitude of the tool generated MSFE peak (A, B, C) and the mean value of all other significant maximums of amplitude in the spatial frequency interval between 0.5 and 4 1/mm (D, E, F) after polishing.

It can be seen that, for smaller wavelengths, the tool generated MSFE decreases more than the average MSFE from other sources. The average MSFE from other sources on the other hand decreases less. For frequencies with longer wavelength, the tool generated MSFE decreases less than the average MSFE from other sources. The average MSFE from other sources on the other hand decreases more. It can be stated that surface structures with smaller spatial wavelengths are better removed by polishing than to structures with longer spatial wavelengths. However, by decreasing the wavelength of the tool generated MSFE, other secondary error sources seem to also decrease in wavelength. As a result, former form errors shrink into the lower MSFE range and the average MSFE decreases less by polishing. Lower path speeds seem to additionally intensify this effect.

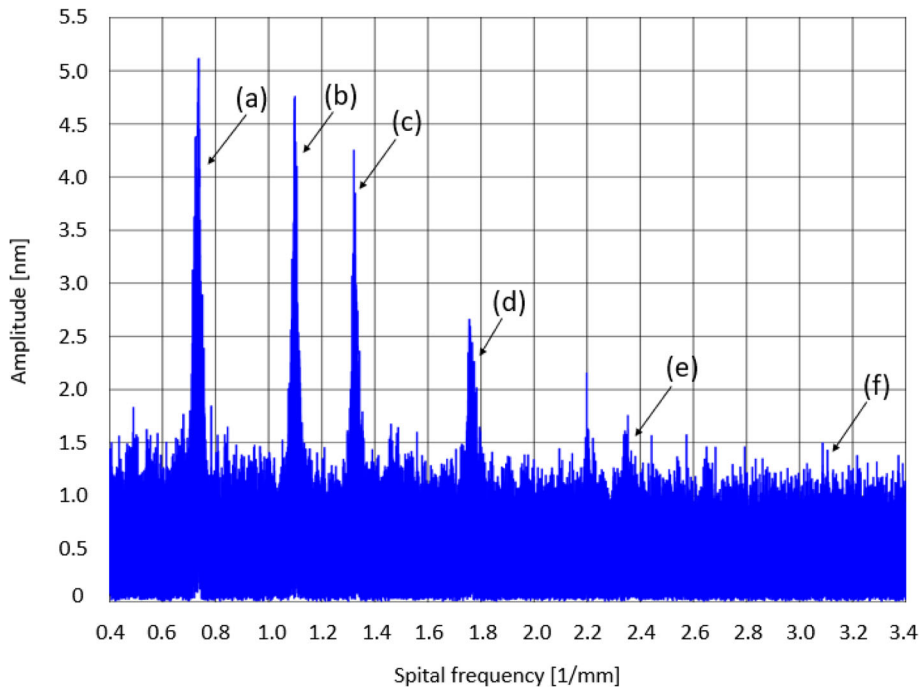


**Fig. 3** Amplitude frequency spectrum (0.4 1/mm < spatial frequency < 3.4 1/mm) of a ground sample. The surface error is displayed as spatial frequencies (1 / mm) and the amplitude is given in nanometres. The frequency peaks are labelled (a, b, c, d, e, and f) according to Table 2. Fourier transformation: Normalized, unity window

It is very difficult to remove the MSFE, therefore the better strategy is to avoid it. The rotation of the tool always leaves a remaining structure on the surface. The ratio between tool rotation and path speed should be chosen in a way to generate small resulting MSFE wavelengths. However, if the tool generated MSFE wavelengths get too small, former form errors shrink their wavelength and enter the MSFE range and the residual MSFE from other sources increases. Therefore, the ratio between tool rotation and path speed should be kept in reasonable boundaries. The resulting MSFE wavelength should be as small as possible but still big enough to prevent form errors from shrinking into

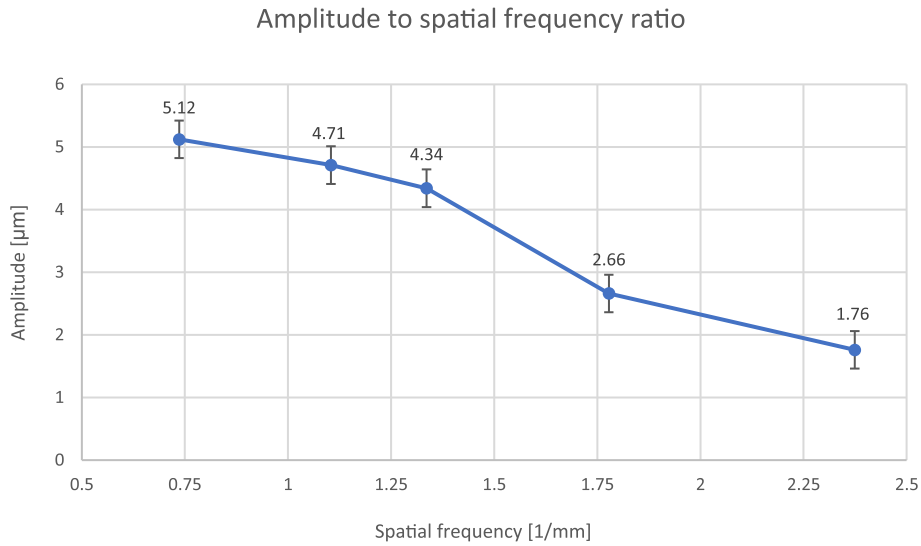


**Fig. 4** Behaviour of the amplitude of the MSFE-Peaks after grinding with respect to its spatial frequency. Due to the constant path speed, higher spatial frequencies resemble higher rotation speeds of the tool (Eqs. 1 and 2). The amplitude value of each datapoint is displayed above the point

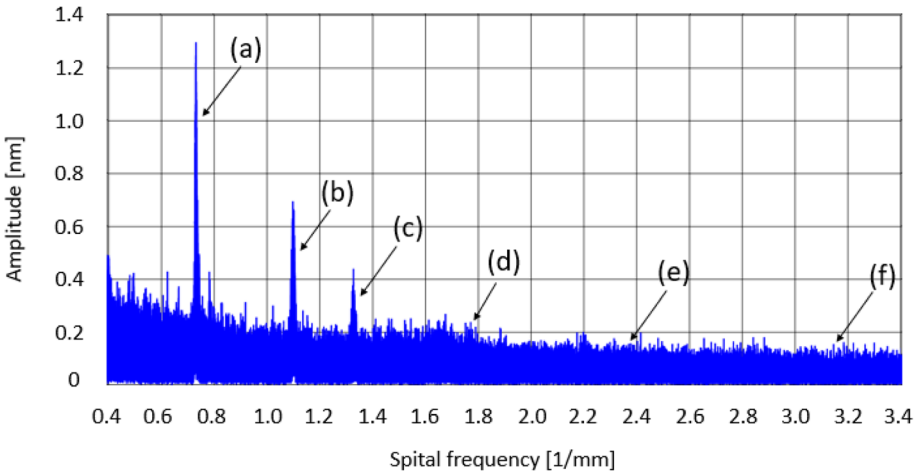


**Fig. 5** Amplitude frequency spectrum (0.4 1/mm < spatial frequency < 3.4 1/mm) of the same sample as displayed in Fig. 5 after polishing. The surface error is displayed as spatial frequencies (1 / mm) and the amplitude is given in nanometres. The frequency peaks are labelled (a, b, c, d, e, and f) according to Table 2. Fourier transformation: Normalized, unity window

the MSFE range due to the acceleration of the rotation speeds and other mechanisms of the grinding machine. In case of the manufacturing process used in this experiments, the best results were achieved with a ratio between tool rotation and path speed, that led to an error wavelength generated by the tool of about 0.4 mm.

## MSFE prevention strategies

Based on these results, it is possible to come up with several strategies to avoid or at least decrease the tool related MSFE during the manufacturing process.

The first and most promising MSFE prevention strategy is an increase in rotation speed of the tool. This also increases the spatial frequency of the error generated by the tool. The spatial frequency can be shifted into the range of roughness and thus removed by the polishing. Even if it cannot be completely shifted into the range of roughness, the polishing process will still decrease the amplitude of the frequency the better, the smaller its wavelength gets. Besides that, the experiments have shown that, the amplitude of the generated frequency generally decreases for higher rotation speeds. Therefore, the increase of the rotation speed of the tool shifts the

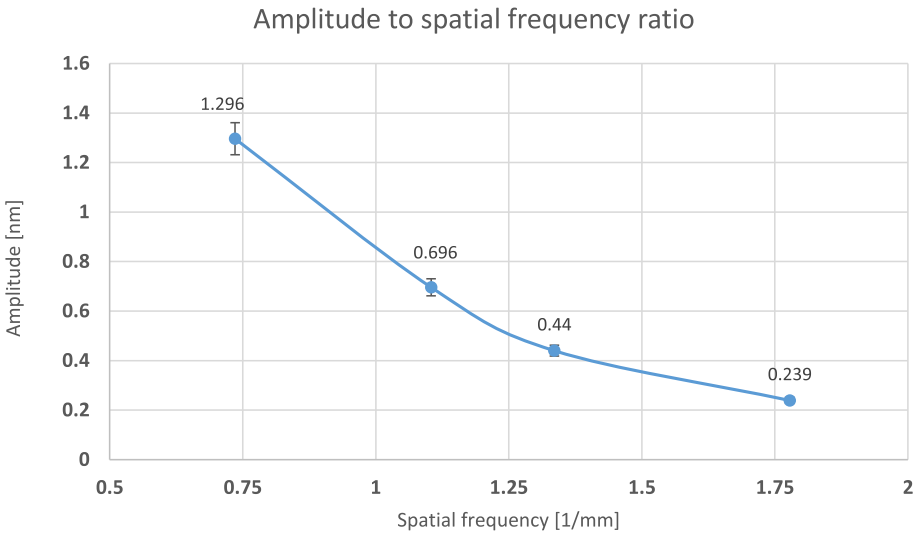


**Fig. 6** Behaviour of the amplitude of the MSFE-Peaks after polishing with respect to its spatial frequency. Due to the constant path speed, higher spatial frequencies resemble higher rotation speeds of the tool (Eqs. 1 and 2). The amplitude value of each datapoint is displayed above the point

**Table 3** Grinding parameters for spherical samples evaluated in Figs. 7 and 8 in order with the resulting spatial frequency peaks and wavelengths

| # Sample | Path speed [mm/min] | Tool rotation [1/min] | Frequency peak [1/mm] | Spatial wavelength [mm] |
|---|---|---|---|---|
| 1 | 2000 | 2207 | 1.1 | 0.91 |
| 2 | | 2671 | 1.3 | 0.77 |
| 3 | | 4751 | 2.4 | 0.42 |
| 4 | | 6277 | 3.1 | 0.32 |
| 5 | 4000 | 4421 | 1.1 | 0.91 |
| 6 | | 5347 | 1.3 | 0.77 |
| 7 | | 9497 | 2.4 | 0.42 |
| 8 | | 12,569 | 3.1 | 0.32 |
| 9 | 6000 | 6619 | 1.1 | 0.91 |
| 10 | | 8017 | 1.3 | 0.77 |
| 11 | | 14,243 | 2.4 | 0.42 |

generated frequency into a range where the polishing process becomes much more effective in decreasing the amplitude. Besides that, the initial amplitude from the grinding process is lower. The disadvantages of this strategy are safety issues due to the higher rotation speeds and other potential side effects. For example, an increase in secondary MSFE sources due to shifting form errors into the MSFE range.

The second MSFE prevention strategy is a decrease in path speed. This would increase the spatial frequency of

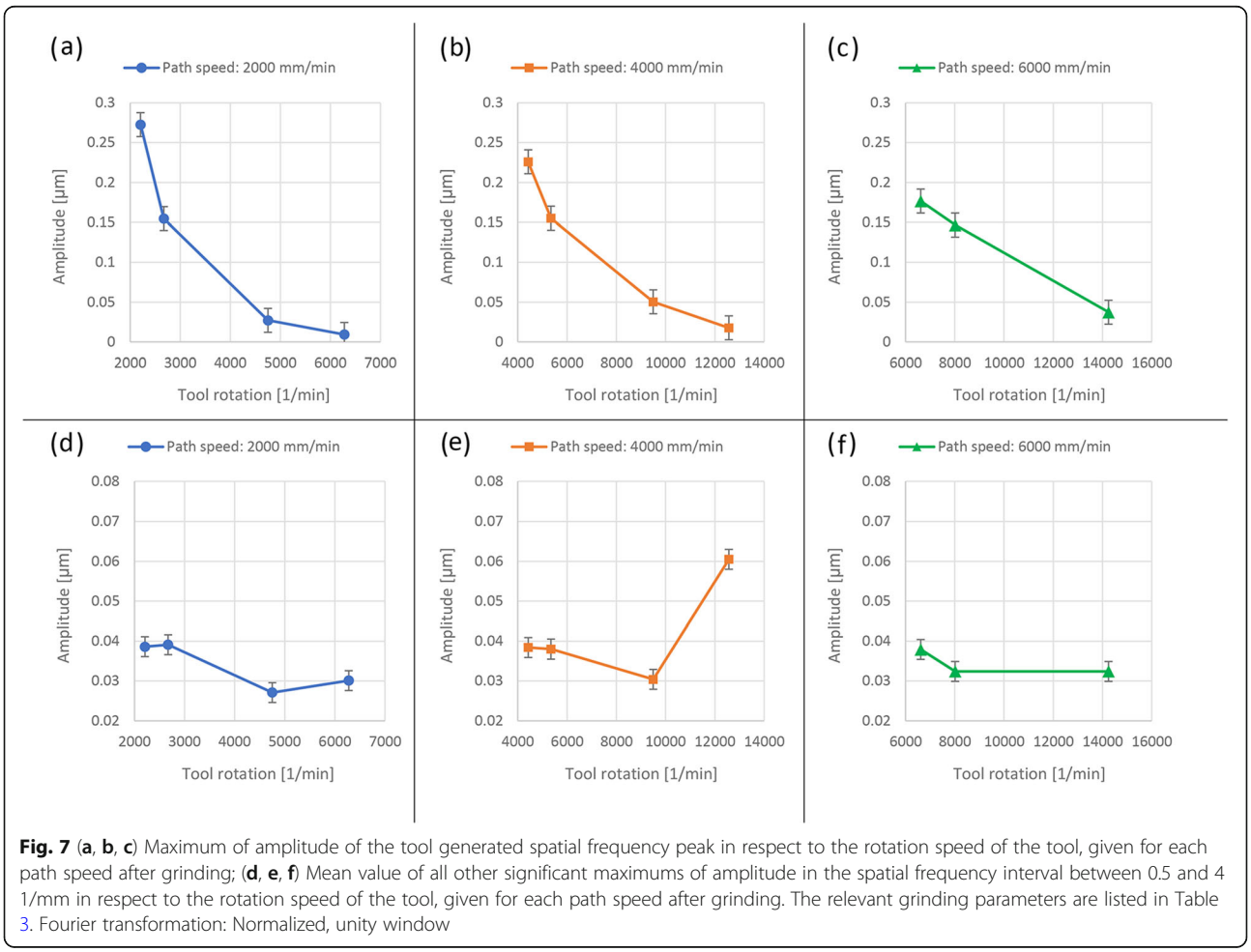


**Fig. 7** (**a**, **b**, **c**) Maximum of amplitude of the tool generated spatial frequency peak in respect to the rotation speed of the tool, given for each path speed after grinding; (**d**, **e**, **f**) Mean value of all other significant maximums of amplitude in the spatial frequency interval between 0.5 and 4 1/mm in respect to the rotation speed of the tool, given for each path speed after grinding. The relevant grinding parameters are listed in Table 3. Fourier transformation: Normalized, unity window

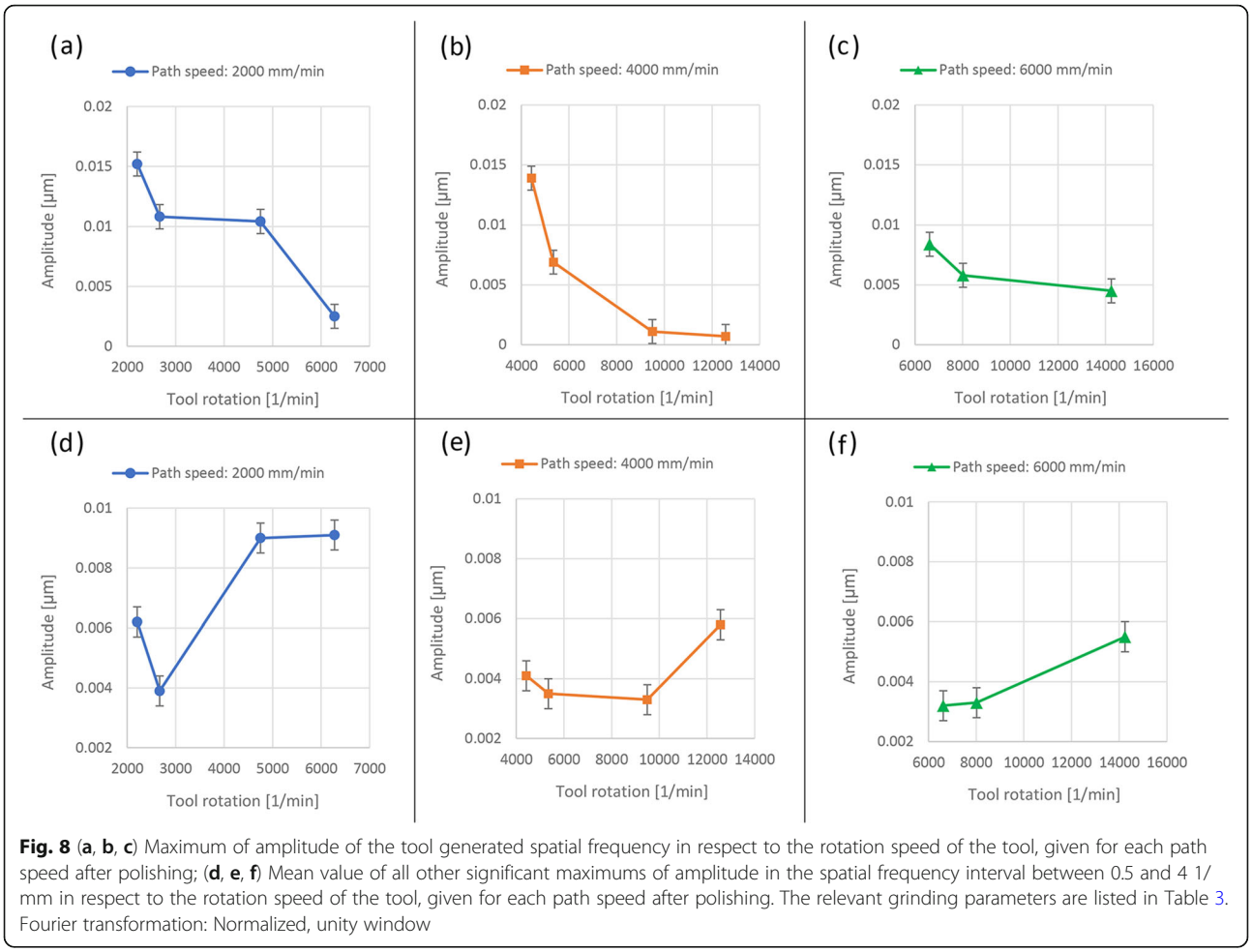


**Fig. 8** (**a**, **b**, **c**) Maximum of amplitude of the tool generated spatial frequency in respect to the rotation speed of the tool, given for each path speed after polishing; (**d**, **e**, **f**) Mean value of all other significant maximums of amplitude in the spatial frequency interval between 0.5 and 4 1/mm in respect to the rotation speed of the tool, given for each path speed after polishing. The relevant grinding parameters are listed in Table 3. Fourier transformation: Normalized, unity window

the error generated by the tool. The spatial frequency can be shifted into the range of roughness and thus removed by the polishing. Even if it cannot be completely shifted into the range of roughness, the polishing process will still decrease the amplitude of the frequency the better, the smaller its wavelength gets. Therefore, the decrease in path speed shifts the generated frequency into a range where the polishing process becomes much more effective in decreasing the amplitude. The disadvantages of this strategy are the increase in manufacturing time due to the lower path speed and an increase in secondary MSFE sources due to shifting form errors into the MSFE range. If the path speed is chosen too low, the shift of form errors into the MSFE range gets intensified.

The third MSFE prevention strategy is to dress and balance the tool. It is impossible to perfectly mount and shape the tool. Therefore, the moment the tool starts rotating, it will start a periodic deflection which can be expressed as the rotation frequency of the tool (1 spin = 1 period). The amplitude of this frequency determines the amplitude of the tool generated MSFE. Consequently, the better the tool is dressed and balanced, the lower the resulting amplitude of the MSFE. The disadvantage of this strategy is that dressing and balancing the tool takes a lot of time, effort and experience.

## Conclusions

The experiments have shown that it is possible to avoid or at least decrease the appearance of the MSFE from the grinding process by adjusting the grinding parameters. To achieve that, three strategies of avoidance were proposed. Which of the proposed strategies are valid, needs to be judged on each individual manufacturing process.

Figure 4 shows that the amplitudes of the generated frequencies are generally decreasing with an increase in rotation speed of the tool. This can be explained by the gyroscopic effect of the grinding tool. Higher rotation speeds stabilize the rotational behaviour of the tool and decrease its radial run-out [15].

In the case of the manufactured sample evaluated in Figs. 3 and 5, the maximums of amplitude seem very low. Compared to that, the amplitudes given in the graphs of Figs. 7 and 8 are much higher. These

differences can be explained by the different normalization of the used fast Fourier transformation (FFT). The amplitudes are normalized by the number of data points along the measurement length. In case of the manufactured sample evaluated in Figs. 3 and 5 each frequency is only obtainable along a certain part of the measurement length. But the amplitudes of the frequencies are normalized to the data points of the whole measurement length. If each parameter section is evaluated separately, the amplitude values of the sample evaluated in Figs. 3 and 5 are comparable to the amplitude values given in the graphs of Figs. 7 and 8.

The theoretical value of the amplitude of the frequency that generates the MSFE should be in the range of half of typical peak to valley values of the MSFE (e.g. Fig. 1). But such an amplitude is too big to be caused by a well-balanced and dressed tool or a state-of-the-art grinding machine. Therefore, the MSFE generation mechanism is a superposition of smaller frequencies.

After the tool has passed a certain point on the tool path, it will pass the point on its next spiral turn with a distance of one spiral path distance. The area the tool affects at once, is much bigger than one spiral path distance. Therefore, on each spiral rotation, the tool also affects the path of previous and future spiral rotations. In case of the tool used in the experiments, the depth of cut h was at 50 μm and the tool radius of curvature r was at 60 mm. According to the circular chord equation (Eq. 3), the width s of the area the tool affects at once is at about 4.9 mm (flat sample). In the case of the sample evaluated in Figs. 3 and 5, the spiral distance of the tool path was at 50 μm. In this case, the tool affects up to 97 adjacent spiral rotations at once.

$$s = 2\sqrt{2rh - h^2} \tag{3}$$

Due to the different length of the spiral turns, the tool frequencies are not aligned in phase on the previous and future spiral turns. The frequencies are phase shifted to each other due to the different spiral rotation length. Besides that, the different spiral turns lead to small decreases and increases, in the generated wavelength, due to the offset of the tool. Additionally, the machine parameters are never perfectly constant during the

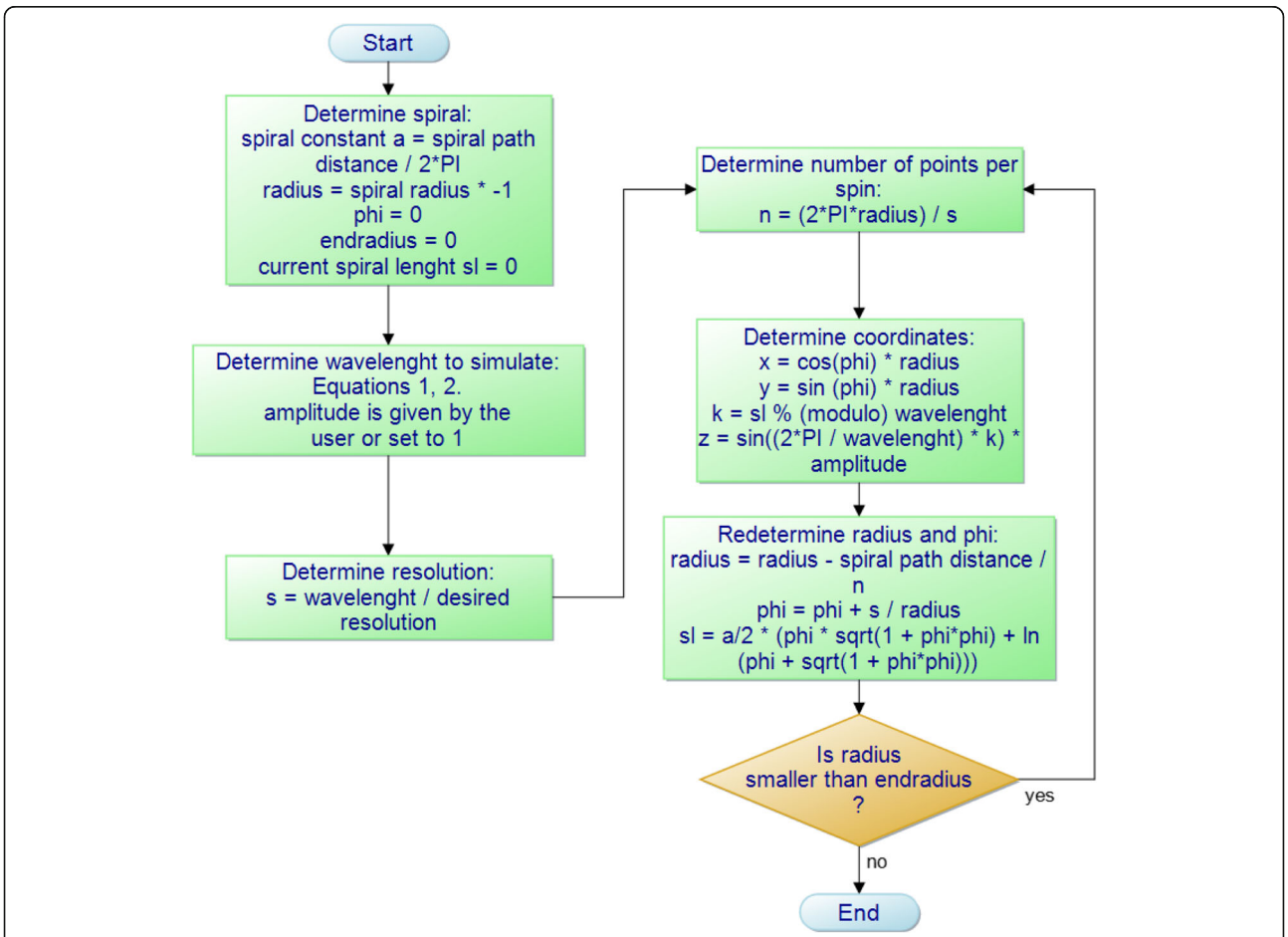


**Fig. 9** Algorithm flow chart for the presented simulation in case of a single frequency, constant path speed and spiral tool path

grinding. The inhomogeneities of the machine parameters also lead to small decreases and increases in the generated wavelength. As a result, the complete tool generated MSFE on the surface of a sample consists of a superposition of similar but slightly different sub frequencies. When several maxima or minima of amplitude concentrate together in one point on the surface, the amplitudes add up and the typical MSFE structures are generated.

This leads to a potential fourth strategy of avoidance. In case of a constant rotation speed of the work piece for example, the rotation speeds can be chosen in a way, that the angle speed of the workpiece divided by tool rotation resembles a factor of 3π or close to it. This way, it could be possible to avoid that several maxima or minima of amplitude from several spiral rotations concentrate together in one point on the surface.

Figure 6 shows that the amplitude of higher spatial frequencies is significantly more decreased by the polishing than the amplitude of lower spatial frequencies. To keep the shape constant during the polishing, typical polishing tools are soft enough to adapt to bigger surface structures. But the tools are also stiff enough to not adapt to small structures and thus remove them. The MSFE's are typically in the border area between adapting and not adapting to it. Therefore, even small decreases in wavelength of the MSFE's can lead to significantly better polishing results.

## Simulation

It is possible to build up a virtual model of the grinding process and overlay it with the main frequency from the grinding step. The main frequency is calculated with Eqs. 1 and 2. This leads to a simulation of the appearance of the MSFE in the grinding process.

The simulation is provided with the grinding parameters and the tool parameters. Afterwards the simulation can be used to simulate MSFE as a single frequency or as a frequency peak. In the second case, it assumes a Gaussian distribution of the frequencies inside a given width around the tool frequency. The amplitude is determined experimentally and given to the simulation. For the purpose of predicting structures, the amplitude is neglected so far. The simulation makes accumulations of minima and maxima of amplitude along the tool path visible. This way, the simulation is also able to predict MSFE structures which result from the superposition of the frequencies. The functional principal of the simulation, in case of a single frequency, constant path speed and spiral tool path is shown in Fig. 9.

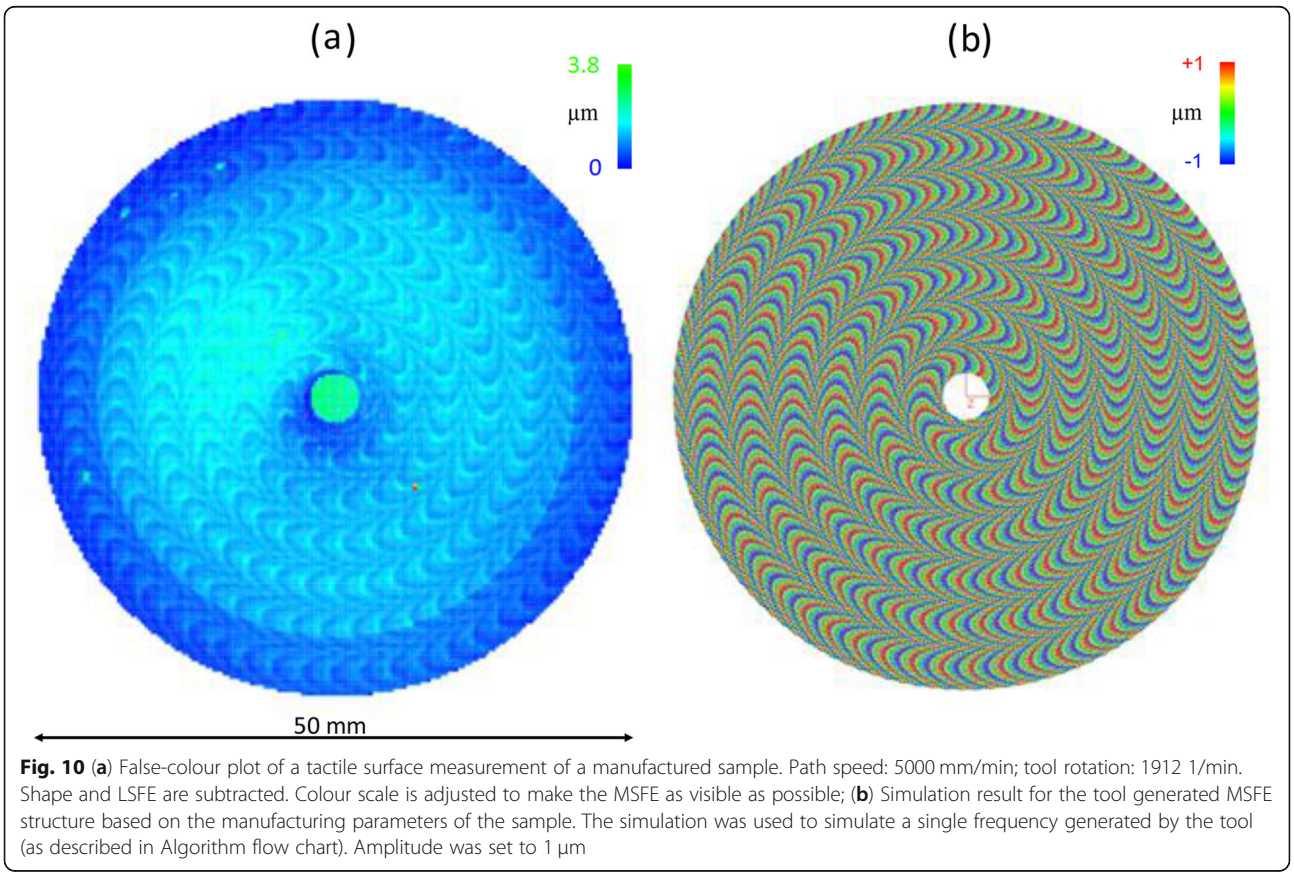


**Fig. 10** (**a**) False-colour plot of a tactile surface measurement of a manufactured sample. Path speed: 5000 mm/min; tool rotation: 1912 1/min. Shape and LSFE are subtracted. Colour scale is adjusted to make the MSFE as visible as possible; (**b**) Simulation result for the tool generated MSFE structure based on the manufacturing parameters of the sample. The simulation was used to simulate a single frequency generated by the tool (as described in Algorithm flow chart). Amplitude was set to 1 µm

The MSFE structure on the surface of a measured sample is a superposition of all frequencies on the surface, including LSFE and HSFE. Besides that, there is also a superposition of frequencies inside the range of the main frequency peak. Because of that, it is very tough to compare the simulation results with the original measurement data by its visual impression. For this reason, revised measurement data is needed. Shape and LSFE were subtracted from the measurement data of a sample. Then its colour scale was adjusted to make the MSFE as visible as possible. Figure 10 shows the revised surface measurement of the real sample (A) and the related simulation result for the MSFE structure (B).

With the revised measurement it is possible to review the simulation results by its visual impression. However, the revision requires time and is not possible for every measurement data. Alternatively, the simulation data can be verified by analysing the simulation results the same way as the measurement and compare their amplitude frequency spectrum.

The simulation is able to correctly predict the grinding tool related MSFE structure based on the grinding parameters. It could be possible to purposely create structures which respond best to a specific polishing technique. Besides that, it could also be possible to purposely create MSFE structures which compensate each other in multi-lens systems. This could make the simulation tool useful for optical design.

### Abbreviations

SSD: Sub surface damages; LSFE: Low-spatial frequency error; MSFE: Mid-spatial frequency error; HSFE: High-spatial frequency error; CCP: Computer controlled polishing; FFT: Fast Fourier transformation

### Acknowledgements

Not applicable.

### Authors' contributions

All authors contributed equally in compiling this review. All authors read and approved the final manuscript.

### Funding

This research (EmmaV) is funded by the German Federal Ministry for Economic Affairs and Energy and several industrial partners under the program of collective industrial research (IGF) (Contract no 18564 N/2). The Author's would like to thank the German Federal Ministry for Economic Affairs and Energy and the industrial partners listed below for funding this research.
The Authors acknowledge funding by:
• German Federal Ministry for Economic Affairs and Energy
• asphericon GmbH
• Berliner Glas KGaA
• Carl Zeiss Jena GmbH
• Carl Zeiss SMT GmbH
• FISBA OPTIK AG
• JENOPTIK Optical Systems GmbH
• Leica Camera AG
• Leica Microsystems GmbH
• Opteg GmbH
• OptoTech Optikmaschinen GmbH
• POG Präzisionsoptik Gera GmbH
• Qioptiq Photonics GmbH & Co. KG
• Satisloh AG
Open access funding provided by Projekt DEAL

### Availability of data and materials

Upon request to the authors.

### Ethics approval and consent to participate

Not applicable.

### Consent for publication

Not applicable.

### Competing interests

The authors declare that they have no competing interests.

### Author details

[1]Aalen University of Applied Sciences, Center for Optical Technologies, 73430 Aalen, Germany. [2]Technical University Deggendorf, Institute for Precision Manufacturing and High-Frequency Technology, 94244 Teisnach, Germany.

Received: 31 January 2020 Accepted: 17 July 2020
Published online: 03 August 2020

### References

1. Vogt, C., Deggendorf, D. E., Mazal, J., Lohner, R.-D.: The cause of structures on ground shapes. In: Proceedings of 3rd EOS Conference on Manufacturing of Optical Components 2013 (EOSMOC 2013). EOS Conferences at the World of Photonics Congress 2013 13 - 15 May 2013, International Congress Centre Munich (ICM), Germany. vol. 1, pp. 97. European Optical Society (EOS), Curran Associates, Inc, (2013)
2. Braunecker, B., Hentschel, R., Tiziani, H.J.: Advanced Optics Using Aspherical Elements. SPIE Press, Washington (2008) ISBN: 9780819467492
3. Aikens, D.M., DeGroote, J.E., Youngworth, R.N.: Specification and control of mid-spatial frequency wavefront errors in optical systems. In: Frontiers in Optics 2008/Laser Science XXIV/Plasmonics and Metamaterials/Optical Fabrication and Testing. Optical Society of America (2008). https://doi.org/10.1364/OFT.2008.OTuA1
4. Filhaber, J.: Mid-spatial-frequency errors: the hidden culprit of poor optical performance. Laser Focus World. **49**(8), 32–3+ (2013)
5. Kim, D.W., Martin, H.M., Burge, J.H.: Control of mid-spatial-frequency errors for large steep aspheric surfaces. In: OSA OF&T, Figuring and Finishing Science OM4D, June 24–28 (2012). https://doi.org/10.1364/OFT.2012.OM4D.1
6. Liao, D., Yuan, Z., Tang, C., Xie, R., Chen, X.: Mid-Spatial Frequency Error (PSD-2) of optics induced during CCOS and full-aperture polishing. J. Eur. Opt. Soc. Rapid Publ. **8**, ISSN 1990-2573 (2013). https://doi.org/10.2971/jeos.2013.13031
7. DeGroote, J., Light, B., Savage, B., Wiederhold, B., Mandina, M.: VIBE™ finishing to remove mid-spatial frequency ripple. Optical Society of America, Optimax Systems Inc., Ontario (2010). https://doi.org/10.1364/OFT.2010.OWE2
8. Tamkin, J.M., Dallas, W.J., Milster, T.D.: Theory of point-spread function artifacts due to structured mid-spatial frequency surface errors. Appl. Opt. **49**(25), 4814–4824 (2010). https://doi.org/10.1364/AO.49.004814
9. Yu, G., Li, H., Walker, D.: Removal of mid spatial-frequency features in mirror segments. J. Eur. Opt. Soc. Rapid Publ. **6**, 11044 (2011). https://doi.org/10.2971/jeos.2011.11044
10. Pohl, M., Börret, R.: Simulation of mid-spatials from the grinding process. J. Eur. Opt. Soc. Rapid. **11**, 16010 (2016). https://doi.org/10.2971/jeos.2016.16010
11. Yu, G., Reynolds, C., Walker, D., Faehnle, O.: Study of footprint variations of CCP considering machine kinematics. Eur. Phys. J. Conf. **215**(24), 05004 (2019). https://doi.org/10.1051/epjconf/201921505004
12. Pohl, M., Börret, R., Kukso, O., Rascher, R.: Simulation of MSF-errors using Fourier transform. In: Fifth European Seminar on Precision Optics Manufacturing (POM) (2018). https://doi.org/10.1117/12.2317484
13. Pohl, M., Bielke, U., Börret, R., Kukso, O., Rascher, R.: Simulation of MSF-errors using Fourier transform. In: Optical Manufacturing and Testing XII, 09.18; 2018. https://doi.org/10.1117/12.2320214
14. Pohl, M., Bielke, U., Börret, R., Kukso, O., Rascher, R.: MSF-Error Prevention Strategies for the Grinding Process, Sixth European Seminar on Precision Optics Manufacturing (POM) (2019). https://doi.org/10.1117/12.2526581
15. Xiong, G.L., Yi, J.M., Zeng, C., Guo, H.K., Li, L.X.: Study of the gyroscopic effect of the spindle on the stability characteristics of the milling system. J. Mater. Process. Technol. **138**(1–3), 379–384 (2003). https://doi.org/10.1016/S0924-0136(03)00102-X

## Publisher's Note